Biochimica et Biophysica Acta 808 (1985) 235–242
Elsevier

BBA 41765

Spin-trap study of the reactions of ferredoxin with reduced oxygen species in pea chloroplasts

John R. Bowyer [a,*] and Patrick Camilleri [b]

[a] *Plant Exploitation and Protection Group, Department of Biochemistry, Royal Holloway College, Egham Hill, Egham, Surrey, TW20 0EX and* [b] *Shell Research Ltd., Sittingbourne Research Centre, Sittingbourne, Kent, ME9 8AG (U.K.)*

(Received November 26th, 1984)

Key words: Superoxide formation; ESR; Ferredoxin; Spin trap; (Pea chloroplast)

Illumination of pea chloroplasts in the presence of the spin trap 5,5-dimethyl-1-pyrroline-*N*-oxide results in the formation of the superoxide spin adduct, an effect enhanced by addition of artificial Photosystem I electron acceptors such as paraquat. Addition of spinach ferredoxin alone slightly enhances superoxide formation, but causes inhibition of superoxide formation when the rate has been increased by added paraquat. This is not accompanied by an inhibition of O_2 uptake, and provides evidence that ferredoxin reduces superoxide to hydrogen peroxide. Decay of the superoxide adduct signal under illumination is not accompanied by the appearance of hydroxyl adduct. This signal, however, appears on cessation of illumination, and disappears on reillumination. This is probably due to conversion of the hydroxyl adduct into a non-radical species by a redox reaction linked to photosynthetic electron transport, since the light-induced decrease in this signal is inhibited by the photosynthetic electron-transport inhibitor 3-(3′,4′-dichlorophenyl)-1,1-dimethylurea. Both Fe^{3+} chelated by diethylenetriaminepentaacetic acid, and spinach ferredoxin, reduced by the photosynthetic electron-transport chain, react with hydrogen peroxide to produce hydroxyl radicals in a Fenton-type process.

Introduction

Illuminated chloroplasts generate superoxide through the reduction of dioxygen by Photosystem I, and the enhancement of this process by the bipyridinium herbicides (e.g., paraquat) and the dioxathiadiaza-2,5-heteropentalene derivatives (e.g., HEP II) is thought to be the first event in their herbicidal action (reviewed in Ref. 1, and see also Refs. 2–6). The physiological Photosystem I electron acceptor ferredoxin has also been shown to be oxidisable by oxygen, generating hydrogen peroxide [7] and ultimately water as the final product (ref. 8 and reviewed in Refs. 9 and 10). Allen [11] has obtained tentative evidence that this process proceeds via intermediate free superoxide, and Hosein and Palmer [12] have tentatively demonstrated that free hydroxyl radicals are generated during the reduction of hydrogen peroxide by ferredoxin. These reactions are important, both because the reduction of superoxide by ferredoxin may serve as a back-up to its removal by superoxide dismutase, and because the generation of toxic hydroxyl radicals in the chloroplast is highly unfavourable.

Superoxide formation has been monitored in chloroplasts using the spin trap 5,5-dimethyl-1-pyrroline-*N*-oxide which reacts with both superoxide and hydroxyl radicals to give relatively

* To whom all correspondence should be addressed.

Abbreviations: HEP II, dioxathiadiaza-2,5-pentalene derivative II (see Refs. 5 and 6); DMPO, 5,5-dimethyl-1-pyrroline-*N*-oxide; DMPO-OOH, DMPO-superoxide spin adduct; DMPO-OH, DMPO-hydroxyl spin adduct; ESR, electron spin resonance; DCMU, 3-(3′,4′-dichlorophenyl)-1,1-dimethylurea; Chl, chlorophyll.

long-lived adducts designated DMPO-OOH and DMPO-OH, respectively, with characteristic ESR spectra [6,13–16]. We have used this technique to study the effect of ferredoxin on superoxide formation in pea chloroplasts in the presence of paraquat or HEP II, and also to study the generation of hydroxyl radicals during the reaction of photoreduced ferredoxin with hydrogen peroxide.

DMPO-OOH has been detected in experiments with chloroplasts and paraquat [6,15,16], but there have been no published spectra indicating a significant presence of DMPO-OH, even though a large amount of DMPO-OH can arise through the decay ($t_{1/2} \approx 60$ s) of DMPO-OOH [17]. We have studied the conditions that can lead to the rapid appearance of DMPO-OH after the complete decomposition of DMPO-OOH.

Materials and Methods

Techniques for the preparation of broken pea chloroplasts and assay for chlorophyll content are described elsewhere [6,18]. For ESR spectroscopy, chloroplasts were suspended to 75 μg/ml chlorophyll in oxygenated 50 mM morpholinopropane sulphonic acid buffer (pH 7) containing 2 mM NH_4Cl/80 mM NaCl/1 mM diethylenetriamine pentaacetic acid/0.2 M DMPO [6]. Other additions are described in the figure legends. 1 ml of this suspension was sucked into an aqueous ESR sample cell and ESR measurements and sample illumination using a fibre optic illuminator were carried out as described in Ref. 6. ESR measurements were performed at room temperature, at a microwave power of 20 mW and a frequency of 9.77 GHz, a magnetic field modulation amplitude of 50 μT at 100 kHz and, unless stated otherwise, at a gain of $4 \cdot 10^5$. Other ESR conditions are described in the figure legends. For measurements of oxygen uptake, chloroplasts were suspended to 50 μg/ml chlorophyll in 50 mM morpholinopropane sulphonic acid buffer (pH 7) containing 2 mM NH_4Cl/80 mM NaCl/1 mM diethylenetriamine pentaacetic acid/1 mM sodium azide/2 mM potassium cyanide. Other additions are described in the text. Oxygen uptake was measured at 20°C using a Clark-type oxygen electrode (Hansatech) illuminated by a 150 W projector filtered by a Kodak Wratten 29 red filter providing 600 $W \cdot m^{-2}$ at the sample. Spinach ferredoxin, prepared essentially according to Ref. 19, was kindly provided by Dr. A. Fentem, Shell Research Ltd., Sittingbourne, U.K. DMPO and diethylenetriamine pentaacetic acid were obtained from Aldrich. Bovine liver catalase and bovine erythrocyte superoxide dismutase were obtained from Boehringer, Mannheim, F.R.G.

Results and Discussion

DMPO-OOH was monitored at a peak in the ESR derivative spectrum, determined by running spectra at various times after illumination (e.g., see Fig. 3B, discussed below). The formation and decay kinetics of DMPO-OOH in illuminated pea chloroplasts under various conditions are shown in Fig. 1. Ferredoxin at 20 μM leads to a very small increase in the rate of superoxide adduct forma-

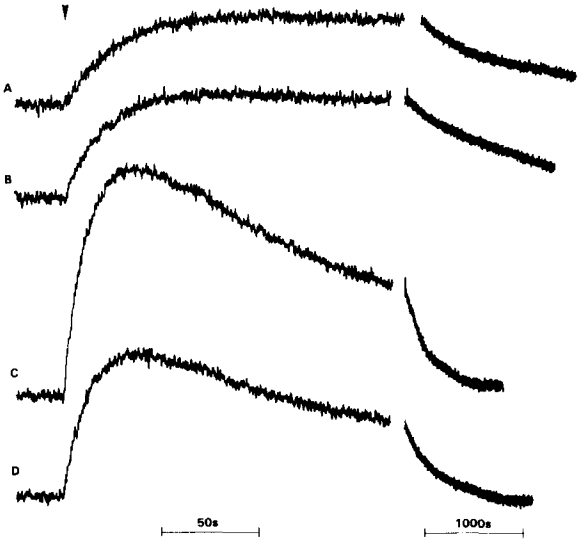

Fig. 1. Kinetics of the formation and decay of DMPO-OOH in illuminated pea chloroplasts. Chloroplasts were suspended in pH 7 buffer as described in Materials and Methods, with the further addition of 20 μM ferredoxin (trace B) or 100 μM paraquat (trace C) or 20 μM ferredoxin with 100 μM paraquat (trace D). Each trace was run on a separate sample. The DMPO-OOH signal was monitored at 0.3464 T, as indicated by the arrow over spectrum B in Fig. 3. The time constants were 200 ms for the rise kinetics and 500 ms for the decay kinetics. Other ESR conditions are described in Materials and Methods. The arrow indicates where the light was turned on. The break in each trace indicates where the pen sweep rate and time constant were switched.

TABLE I

EFFECTS OF FERREDOXIN AND PARAQUAT ON THE INITIAL RATES OF DMPO-OOH FORMATION AND OXYGEN UPTAKE IN ILLUMINATED PEA CHLOROPLASTS

The DMPO-OOH formation rates were measured as described in Materials and Methods in the absence of cyanide and azide. Relative rates measured in the presence of cyanide and azide are 24.5 with 100 μM paraquat, and 11.4 with 100 μM paraquat and 20 μM ferredoxin (Fig. 2). The oxygen uptake rates were measured as described in Materials and Methods in the presence of cyanide and azide. The absence of cyanide had no effect on the rate, but azide must be included to inhibit catalase which otherwise releases O_2 from H_2O_2.

Addition	Relative rate of DMPO-OOH formation	Rate of oxygen uptake (μmol O_2· mg Chl per h)	Relative rate of oxygen uptake
Control	1.00	24.4	1.00
1 μm Paraquat	3.48	99.5	4.07
10 μM Paraquat	5.93	160.6	6.57
100 μM Paraquat	8.07	151.9	6.21
20 μM Ferredoxin	1.66	64.6	2.64
1 μM Paraquat, 20 μM ferredoxin	1.83	172.9	7.07
10 μM Paraquat, 20 μM ferredoxin	–	172.9	7.07
100 μM Paraquat, 20 μM ferredoxin	3.75	172.9	7.07

tion (Fig. 1B and Table I). In contrast, addition of paraquat or HEP II (not shown) leads to considerable increases in the rate of superoxide adduct formation (Fig. 1C and Table I). However, ferredoxin markedly diminishes the initial rate of superoxide adduct formation stimulated by either paraquat or HEP II (Fig. 1D and Table I).

The rates of oxygen uptake and DMPO-OOH formation under various conditions are shown in Table I. The relative initial rates of DMPO-OOH formation do not follow the same pattern as the relative rates of O_2 uptake. It is notable that ferredoxin stimulates oxygen uptake to a much greater extent than DMPO-OOH formation, and, also, that its inhibition of DMPO-OOH formation in the presence of paraquat is not accompanied by an inhibition of oxygen uptake. The simplest interpretation of these results is that ferredoxin reduces superoxide generated by the reaction of oxygen with either reduced paraquat, or reduced ferrodoxin, confirming the suggestions in Refs. 11 and 12. It is also consistent with the failure to detect superoxide directly by rapid kinetic ESR when reduced ferredoxin is mixed with oxygenated buffer solutions [20]. The possibility that the ferredoxin preparation was contaminated with copper-zinc superoxide dismutase was ruled out by studying the formation of DMPO-OOH in the presence of KCN, which inhibits this enzyme. KCN stimulated formation of DMPO-OOH in the presence of both paraquat (Fig. 2A) and ferredoxin (not shown), presumably owing to inhibition of endogenous superoxide dismutase activity (see also Ref. 6), which otherwise competes with the spin trap for superoxide. However, the inhibition by ferredoxin of DMPO-OOH formation in the presence of paraquat was still observed (Fig. 2B). This experiment was carried out in the presence of sodium azide, which inhibits catalase, in order to make it directly comparable with the oxygen uptake measurements. Similar results were obtained in the absence of azide. It is highly unlikely that the ferredoxin was contaminated with cyanide-insensitive superoxide dismutase activity, since this activity appears to be associated with membranous or particulate fractions [21].

The fact that this effect of ferredoxin is seen with both paraquat and HEP II, molecules differing considerably in charge properties, implies that a direct interaction with ferredoxin is not involved. Given that the stromal concentration of ferredoxin is about 1 mM [22], it might be expected that ferredoxin plays an important role in protection against superoxide accumulation.

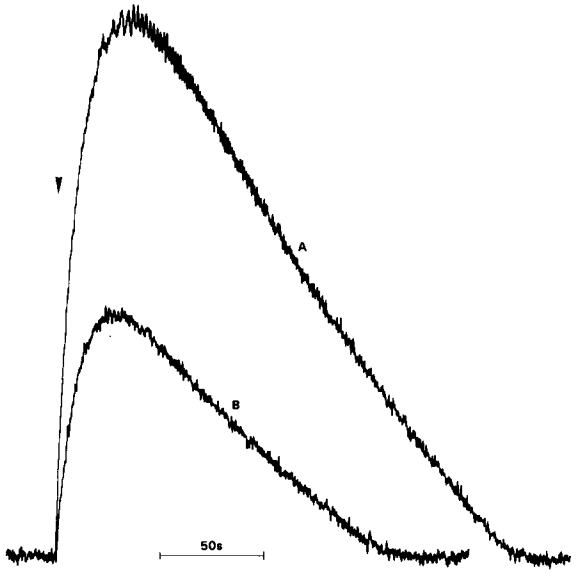

Fig. 2. Effect of ferredoxin on the light-induced formation of DMPO-OOH in the presence of potassium cyanide. Chloroplasts were suspended in pH 7 buffer as described in Materials and Methods, with the further addition of 2 mM potassium cyanide and 1 mM sodium azide, and with 100 μM paraquat (trace A) and 100 μM paraquat with 20 μM ferredoxin (trace B). Each trace was run on a separate sample. The DMPO-OOH signal was monitored as in Fig. 1, with a time constant of 200 ms. The arrow indicates where the light was turned on.

It is clear from Figs. 1 and 2 than an increased rate of formation of DMPO-OOH was accompanied by an increased rate of signal loss under illumination. Signal loss is attributed to decay of DMPO-OOH ($t_{1/2} \approx 60$ s [17]) following depletion of oxygen in the illuminated portion of the ESR flat cell. Steady-state levels of DMPO-OOH were maintained at low rates of oxygen consumption (i.e., at lower light intensities or at lower concentrations of electron acceptor). The accelerated decay of the DMPO-OOH signal seen in the kinetic traces in Fig. 2 in comparison to Fig. 1 is attributed to a more rapid depletion of oxygen resulting from the inhibition of superoxide dismutase and catalase activities, which would otherwise release oxygen from its reduction products.

The spectrum in Fig. 3B is largely attributable to DMPO-OOH (cf. Figs. 1A and 4A in Ref. 14) with minor contributions from an unknown component and from DMPO-OH (seen in the lowest-field minor peak and highest-field minor trough). Thus, the kinetic trace in Fig. 2A and the spectrum

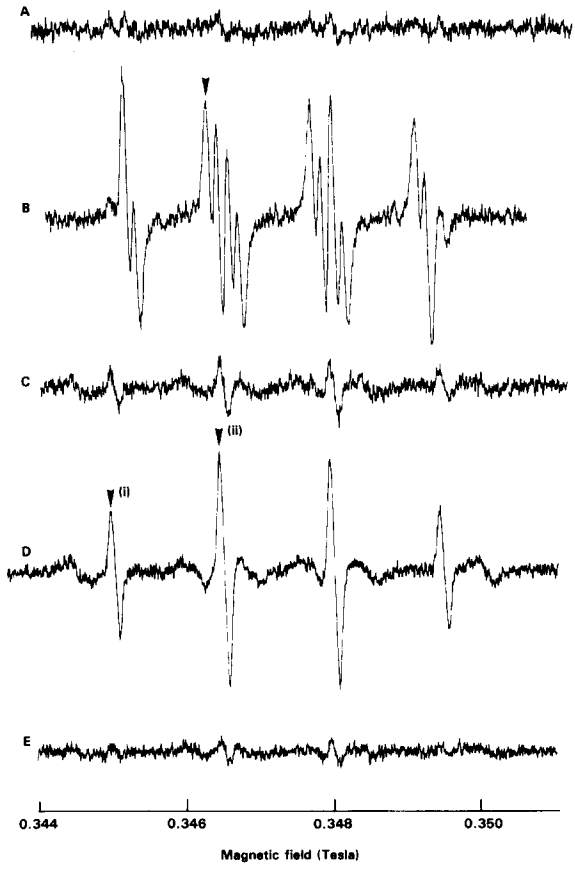

Fig. 3. ESR spectra of DMPO spin adducts under various conditions. Chloroplasts were suspended in pH 7 buffer as described in Materials and Methods, with the further addition of 17 μM ferredoxin. Spectra (A)–(E) were recorded from the same sample: (A) before illumination, (B) in the light after 2.5 min illumination (cf. trace A in Fig. 4), (C) in the light after 30 min illumination, (D) in the dark after 4 min darkness, following 32 min illumination (see trace B in Fig. 4), (E) after the light had been turned back on for 2 min following 10 min in darkness (see trace C in Fig. 4). Spectrum (E) was therefore recorded 44 min after the light was initially turned on. The time at which each spectrum was recorded is the elapsed time between the start of the first period of illumination, and the start of the spectral scan. This may be summarised as follows, where downward arrows indicate light on, and upward arrows indicate light off.

Time (min)		0	2.5	30	32	36	42	44
		↓			↑		↓	
Spectrum	A		B	C		D		E

Spectra were scanned at 0.1 $mT \cdot s^{-1}$ at a time constant of 100 ms. Other ESR conditions are as described in Materials and Methods.

in Fig. 3C confirm that no DMPO-OOH was present after 30 min illumination. The spectrum in Fig. 3D is largely attributable to DMPO-OH (cf. Fig. 1B in Ref. 14), so that spectrum C also shows that very little DMPO-OH was present after 30 min illumination. Spectra recorded at various times during the formation and decay of DMPO-OOH (not shown) confirmed the near absence of DMPO-OH. This is in contrast to the result obtained when DMPO-OOH is generated by the reaction of tetramethylammonium superoxide with DMPO, which indicates that a significant amount of DMPO-OH is apparently produced by the trapping of $OH^{\cdot}$ generated as a breakdown product of DMPO-OOH [17,23].

However, when the light was turned off, the DMPO-OH signal appeared ($t_{1/2} \approx 40$ s) (Figs. 3D and 4B), and subsequently decayed very slowly (a half-time of 14.5 min at pH 7 has been reported [24]). The signal rapidly disappeared when the light was turned back on ($t_{1/2} \approx 6$ s) (Figs. 3E and 4C), and reappeared, although at a smaller amplitude, when the light was again turned off (Fig. 4D). The appearance of the DMPO-OH signal in the dark and its disappearance on re-illumination were seen in the presence of either ferredoxin or paraquat.

In order to test whether photosynthetic electron transport is involved in the disappearance of DMPO-OH in the light, 1 ml samples of chloroplasts prepared for ESR spectroscopy as described in Materials and Methods were illuminated in test tubes for 10 min, sufficient time to generate a significant level of the breakdown products of DMPO-OOH. In the subsequent dark period, any remaining DMPO-OOH decayed. The photosynthetic electron-transport inhibitor DCMU was added to one sample before it was sucked into the ESR cavity and reilluminated. In both control and DCMU-containing samples, a spectrum recorded before reillumination indicated the presence of DMPO-OH at a level similar to that indicated in Fig. 3D, but not DMPO-OOH. On reillumination, approx. 70% of the DMPO-OH rapidly disappeared ($t_{1/2} \approx 3$ s) in the absence of DCMU (trace A in Fig. 5). This process was dramaticlly inhibited by DCMU (trace B in Fig. 5). It seems likely, therefore, that DMPO-OH is converted from a nitroxide into a non-radical species by a redox reaction, probably a reduction linked to photosynthetic electron transfer, and that this reaction is reversed in darkness. A reduction of nitroxides by cytochrome P-450 in rat liver microsomes has been previously reported [25].

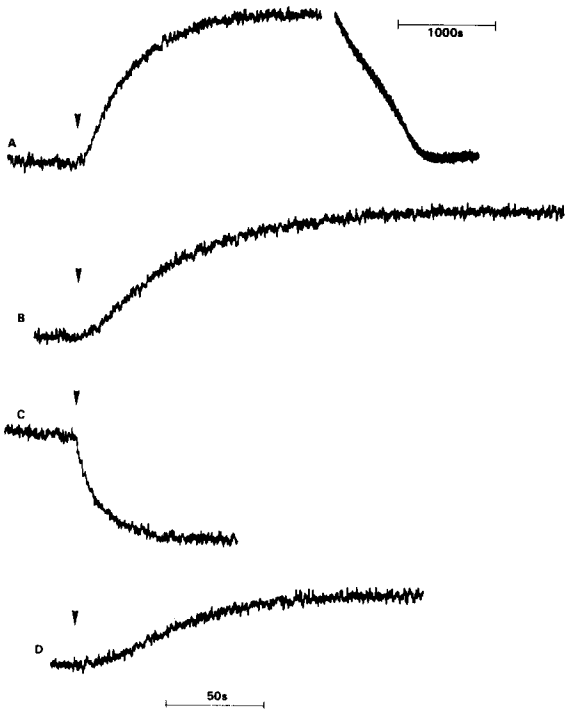

Fig. 4. Kinetics of the appearance and disappearance of DMPO spin adducts under various conditions. Pea chloroplasts were suspended in pH 7 buffer as described in Materials and Methods, with the addition of 17 μM ferredoxin. Traces A–D were recorded on the same sample as that used for spectra A–E in Fig. 3. The DMPO-OH signal was monitored at 0.3465 T as indicated by arrow (ii) over spectrum D in Fig. 3, at a time constant of 200 ms. The DMPO-OOH signal was monitored as in Fig. 1. Other ESR conditions are described in Materials and Methods. The arrows indicate where the light was turned off (traces B and D) or on (traces A and C). Trace A shows the kinetics of appearance of DMPO-OOH when the light is turned on (see spectrum B in Fig. 3), and subsequent disappearance under illumination (see spectrum C in Fig. 3). Trace B shows the kinetics of appearance of the DMPO-OH signal when the light is turned off following 32 min illumination (see spectra C and D in Fig. 3, which were recorded before and after this kinetic measurement). Trace C shows the kinetics of disappearance of the DMPO-OH signal when the light is turned back on after 10 min in darkness (see spectra D and E in Fig. 3, which were recorded before and after this kinetic measurement). Trace D shows the kinetics of reappearance of the DMPO-OH signal when the light is turned off after a further 5 min illumination (during which time spectrum E in Fig. 3 was scanned).

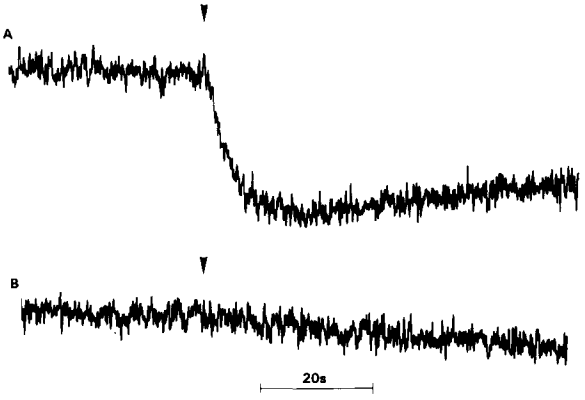

Fig. 5. Effect of DCMU on the light-induced disappearance of the DMPO-OH signal. Chloroplasts were suspended in pH 7 buffer as described in Materials and Methods, with the further addition of 17 μM ferredoxin. 1 ml of suspension was illuminated for 10 min using the same light source as that used to illuminate samples in the ESR cavity. The sample was then sucked in darkness into the ESR cavity and a spectrum was recorded (not shown). The magnetic field was set at 0.3450 T in order to monitor changes in the level of DMPO-OH with a minimum contribution from DMPO-OOH (arrow (i) in Fig. 3D). The arrows over the traces indicate where the light was turned on, 18.5 min after the start of the initial illumination period (i.e., after 8.5 min darkness). For trace B, DCMU was added to 10 μM after the 10 min preillumination, but before the sample was sucked into the ESR cavity. Both traces were recorded at a time constant of 100 ms and a gain of $6.3 \cdot 10^5$.

It is noticeable in trace A, Figure 5, that the rapid light-induced decrease in DMPO-OH is followed by a slower increase. This increase could be dramatically accelerated by the addition of superoxide dismutase, leading to a net doubling of the level of DMPO-OH in the light, in the absence of any DMPO-OOH, which would otherwise decompose to produce DMPO-OH. This preliminary result was taken as tentative support for the suggestion by Hosein and Palmer [12] that reduced ferredoxin reacts with H_2O_2 to generate $OH^{\cdot}$, with the enhancement by superoxide dismutase attributed to removal of superoxide, which would otherwise compete with H_2O_2 for reduced ferrodoxin, and the generation of H_2O_2, the proposed substrate for $OH^{\cdot}$ formation:

$$Fd(II) + H_2O_2 \rightleftharpoons Fd(III) + OH^{\cdot} + OH^-$$

In order to study this process further, chloroplasts were illuminated in the ESR cavity in the presence of H_2O_2, ferredoxin, superoxide dismutase (to remove $O_2^{\cdot-}$ and prevent DMPO-OOH formation) and azide (to inhibit contaminating catalase). This resulted in a steady rate of formation of DMPO-OH (Table II) which was inhibited by the hydroxyl radical scavengers formate (50 mM) and mannitol (140 mM), the former leading to the formation of trapped $CO_2^{\cdot-}$ [23]. The extent of inhibition was increased by lowering the concentration of the competing trap DMPO. DMPO-OH formation was also inhibited by the absence of ferredoxin and by the absence of added hydrogen peroxide and azide.

TABLE II

EFFECT OF FERREDOXIN, $FeCl_3$ AND DETAPAC ON THE INITIAL RATE OF DMPO-OH FORMATION IN ILLUMINATED PEA CHLOROPLASTS

The control contained chloroplasts to 75 μg/ml chlorophyll in pH 7 buffer, 2 mM NH_4Cl, 80 mM NaCl, 0.1 M DMPO, 0.83 mM H_2O_2, 2 mM sodium azide and 150 units/ml superoxide dismutase

Treatment	Relative rate
Control	1.0
20 μM Ferredoxin	4.1
2 μM Heat-treated ferredoxin	2.0
20 μM Ferredoxin, 50 mM formate	2.8
20 μM Ferredoxin, 1300 units/ml catalase, no H_2O_2	0.0
20 μM Ferredoxin, 10 μM DCMU	< 0.08
40 μM $FeCl_3$	0.8
1 mM DETAPAC	2.5
20 μM Ferredoxin, 1 mM DETAPAC	19.1
20 μM Heat-treated ferredoxin, 1 mM DETAPAC	22.7
20 μM Ferredoxin, 1 mM DETAPAC, 50 mM formate	8.2
20 μM Ferredoxin, 1 mM DETAPAC, 1300 units/ml catalase, no H_2O_2	0.2
20 μM Ferredoxin, 1 mM DETAPAC, 140 mM mannitol	6.7
40 μM $FeCl_3$, 1 mM DETAPAC	47.4
40 μM $FeCl_3$, 10 mM DETAPAC	91.9

These reactions were initially performed in the presence of 1 mM DETAPAC, in the hope that it would chelate free Fe^{3+} and prevent its photoreduction, since the chelation of Fe^{3+} by DETAPAC greatly slows its reduction by $O_2^{\cdot-}$ (Ref. 26 and Halliwell, B., personal communication). However, the rate of $OH^{\cdot}$ formation in the presence of 40 μM $FeCl_3$ and 1 mM DETAPAC was much greater than that observed with 20 μM ferredoxin (with 2

Fe per molecule), and increased with increasing concentrations of DETAPAC (Table II). In the absence of DETAPAC, ferredoxin and $FeCl_3$, the rate of formation of DMPO-OH was greatly diminished (Table II) and was only maintained for 80 s (Trace D in Fig. 6). Addition of $FeCl_3$ in the absence of DETAPAC no longer stimulated DMPO-OH formation (in fact, there was a slight inhibition – see Table II), but a stimulation was observed with ferredoxin, although considerably less than that observed with ferredoxin and DETAPAC (Table II and spectrum B in Fig. 7). DMPO-OH formation was distinctly biphasic (Trace A in Fig. 6). Formate slowed the rate of the fast phase, but not that of the slow phase (Trace B in Fig. 6) and trapped $CO_2^{\cdot-}$ was detected (spectrum C in Fig. 7). Heating the concentrated ferredoxin solution (0.17 mM) for 5 min at 100°C before the experiment resulted in a slowing of both the fast and slow phases of DMPO-OH formation,

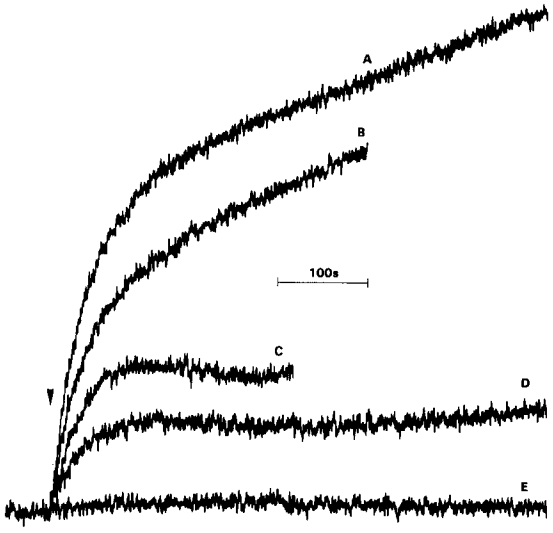

Fig. 6. Kinetics of the formation of DMPO-OH in illuminated pea chloroplasts. Chloroplasts were suspended in pH 7 buffer as described in Materials and Methods, except that no DETAPAC was added, and DMPO was added to 0.1 M. Further additions were to give 0.83 mM H_2O_2 and 2 mM sodium azide (traces A–D), 150 units/ml superoxide dismutase (traces A–E), 1300 units/ml catalase (trace E), 20 μM ferredoxin (traces A, B and E), 20 μM ferredoxin boiled for 5 min (trace C), and 50 mM sodium formate (trace B). The DMPO-OH signal was monitored at 0.3451 T, as indicated by the arrow over spectrum B in Fig. 7. The time constant was 500 ms and the gain was $1 \cdot 10^6$. Other ESR conditions are described in Materials and Methods. The arrow indicates when the light was turned on.

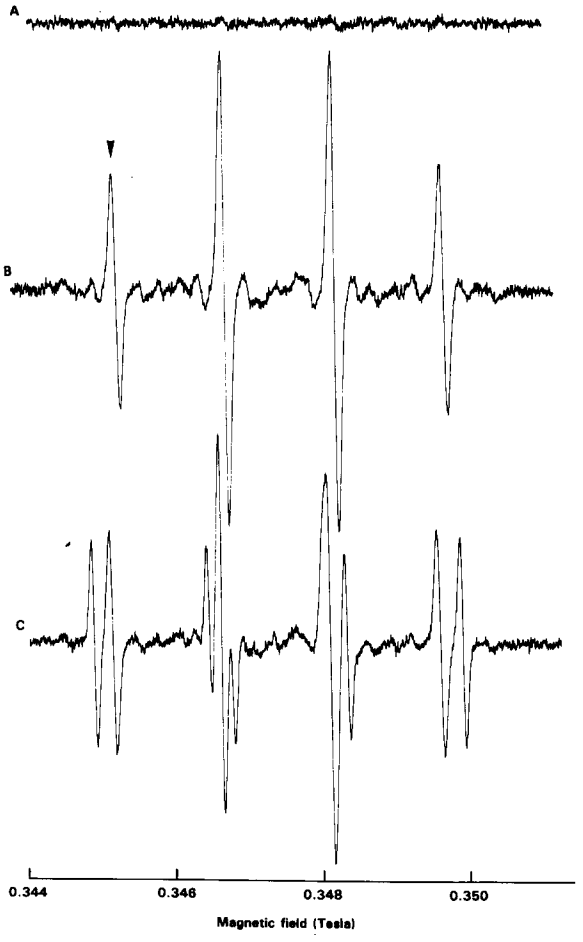

Fig. 7. ESR spectra of DMPO spin adducts under various conditions. Chloroplasts were suspended as in Fig. 6 with the addition of 0.83 mM H_2O_2, 2 mM sodium azide, 150 units/ml superoxide dismutase and 20 μM ferredoxin (traces A–C) and with 50 mM sodium formate (trace C). Spectrum A was recorded in the dark, and spectra B and C were recorded 7.5 min after the onset of illumination. Spectra were scanned at 0.05 $mT \cdot s^{-1}$ at a time constant of 100 ms, and a gain of $3.2 \cdot 10^5$. Other ESR conditions are described in Materials and Methods.

although a slow phase began 4 min after the onset of illumination (trace C and see also trace D in Fig. 6). Formation of DMPO-OH was also inhibited by DCMU. It should, of course, be borne in mind that the rates of DMPO-OH formation may be lowered by the putative photoreduction of DMPO-OH noted earlier.

We interpret these observations as indicating that photoreduced ferredoxin reacts in a Fenton-type process [27] with hydrogen peroxide to generate hydroxyl radicals. Added Fe^{3+} is not effective

in this process, probably because it is not photoreduced, since it is known that Fe^{2+} reacts rapidly with H_2O_2 to produce $OH^{\cdot}$ [27]. DETAPAC chelates Fe^{3+}, facilitating its photoreduction, and Fe^{2+}-DETAPAC reacts with H_2O_2 to produce $OH^{\cdot}$ (Halliwell, B., personal communication). The reduction of Fe^{3+}-DETAPAC by liver microsomal P-450, and its subsequent reoxidation by H_2O_2 generating $OH^{\cdot}$ has been recently reported [28–30].

The DMPO-OH formation seen with heat-treated ferredoxin may reflect incomplete denaturation, but the origin of the biphasic kinetics of formation of DMPO-OH is not yet known. The absence of an effect of formate on the slow phase suggests that the two phases may reflect $OH^{\cdot}$ formation at two different sites, one of which is inaccessible to formate, but not to DMPO. The stimulation of DMPO-OH formation by DETAPAC in the presence of ferredoxin may reflect available Fe^{3+} in the ferredoxin solution, or an interaction of the chelator with the protein-bound 2Fe-2S cluster that facilitates its reaction with H_2O_2.

The demonstration of a reaction between ferredoxin and H_2O_2, producing $OH^{\cdot}$, confirms the result of Hosein and Palmer [12], and indicates that the ability of photoreduced ferredoxin to generate ethylene from methionine in the presence of hydrogen peroxide [31] could be due to hydroxyl radical formation rather than to reaction with a reduced ferredoxin-H_2O_2 complex. The ability of ferredoxin to generate hydroxyl radicals is potentially detrimental, and is presumably normally avoided in vivo through the removal of hydrogen peroxide by ascorbate peroxidase [32], or by a non-destructive reduction of hydroxyl radicals by ferredoxin itself [8,12].

Acknowledgements

We would like to thank Tony Fentem for generously providing spinach ferredoxin.

References

1 Rabinowitch, H.D. and Fridovich, I. (1983) Photochem. Photobiol. 37, 679–690
2 Summers, L.A. (1980) The Bipyridinium Herbicides, pp. 316–319, Academic Press, London
3 Dodge, A.D. (1977) Herbicides and Fungicides – Factors Affecting Their Activity (McFarlane, N.R., ed.), p. 7, The Chemical Society, London
4 Farrington, J.A., Ebert, M., Land, E.J. and Fletcher, F. (1973) Biochim. Biophys. Acta 314, 372–381
5 Camilleri, P., Bowyer, J.R., Clark, M.T. and O'Neill, P. (1984) Biochim. Biophys. Acta 765, 236–238
6 Bowyer, J.R., Camilleri, P. and Stapleton, A. (1984) FEBS Lett. 172, 239–244
7 Telfer, A., Cammack, R. and Evans, M.C.W. (1970) FEBS Lett. 10, 21–24
8 Arnon, D.I., Tsujimoto, H.Y. and McSwain, B.D. (1964) Proc. Natl. Acad. Sci. USA 51, 1274–1282
9 Allen, J.F. (1981) in Commentaries in Plant Science, Vol. 2 (Smith, H., ed.), pp. 97–107, Pergamon Press, Oxford
10 Allen, J.F. (1977) in Superoxide and Superoxide Dismutases (Michelson, A.M., McCord, J.M. and Fridovich, I., eds.) pp. 417–436, Academic Press, New York
11 Allen, J.F. (1975) Biochem. Biophys. Res. Commun. 66, 36–43
12 Hosein, B. and Palmer, G. (1983) Biochim. Biophys. Acta 723, 383–390
13 Green, M.R., Hill, H.A.O., Okolow-Zubkowska, M.J. and Segal, A.W. (1979) FEBS Lett. 100, 23–26
14 Finkelstein, E., Rosen, G.M. and Rauckman, E.J. (1980) Arch. Biochem. Biophys. 200, 1–16
15 Harbour, J.R. and Bolton, J.R. (1975) Biochem. Biophys. Res. Commun. 64, 803–807
16 Chia, L.S., McRae, D.G. and Thompson, J.E. (1982) Physiol. Plant. 56, 492–499
17 Finkelstein, E., Rosen, G.M., Rauckman, E.J. and Paxton, J. (1979) Mol. Pharmacol. 16, 676–685
18 Arnon, D.I. (1949) Plant Physiol. 24, 1–15
19 Rao, K.K., Cammack, R., Hall, D.O. and Johnson, C.E. (1971) Biochem. J. 122, 257–265
20 Orme-Johnson, W.H. and Beinert, H. (1969) Biochem. Biophys. Res. Commun. 36, 905–911
21 Jackson, C.J., Dench, J., Moore, A.L., Halliwell, B., Foyer, C.H. and Hall, D.O. (1978) Eur. J. Biochem. 91, 339–344
22 Lilley, R. McC. and Walker, D.A. (1979) in Encyclopedia of Plant Physiology, New Series Vol. 6, Photosynthesis II (Gibbs, M. and Latzko, E., eds.) pp. 41–53, Springer Verlag, Berlin
23 Finkelstein, E., Rosen, G.M. and Rauckman, E.J. (1981) Mol. Pharmacol. 21, 262–265
24 Marriott, P.R., Perkins, M.J. and Griller, D. (1980) Can. J. Chem. 58, 803–807
25 Rosen, G.M., Rauckman, E.J. and Hanck, K.W. (1977) Toxicol. Lett. 1, 71–74
26 Halliwell, B. (1978) FEBS Lett. 92, 321–326
27 Walling, C. (1975) Acc. Chem. Res. 8, 125–131
28 Ingelman-Sundberg, M. and Johansson, I. (1984) J. Biol. Chem. 259, 6447–6458
29 Morehouse, L.A., Thomas, C.E. and Aust, S.D. (1984) Arch. Biochem. Biophys. 232, 366–377
30 Winston, G.W., Feierman, D.E. and Cederbaum, A.I. (1984) Arch. Biochem. Biophys. 232, 378–390
31 Elstner, E.F., Saran, M., Bors, W. and Lengfelder, E. (1978) Eur. J. Biochem., 89, 61–66
32 Nakano, Y. and Asada, K. (1980) Plant Cell Physiol. 21, 1295–1307